Renewable Energy 132 (2019) 167–175

Contents lists available at ScienceDirect

Renewable Energy

journal homepage: www.elsevier.com/locate/renene

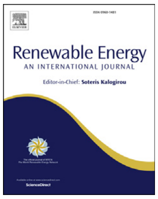

Improved hydrogen storage dynamics of amorphous and nanocrystalline Ce-Mg-Ni-based $CeMg_{12}$-type alloys synthesized by ball milling

Yanghuan Zhang [a, b, *], Wei Zhang [a, b], Wengang Bu [b], Ying Cai [a], Yan Qi [b], Shihai Guo [b]

[a] Key Laboratory of Integrated Exploitation of Baiyun Obo Multi-Metal Resources, Inner Mongolia University of Science and Technology, Baotou 014010, PR China
[b] Department of Functional Material Research, Central Iron and Steel Research Institute, Beijing 100081, PR China

ARTICLE INFO

Article history:
Received 8 March 2018
Received in revised form
18 June 2018
Accepted 29 July 2018
Available online 1 August 2018

Keywords:
$CeMg_{12}$ alloy
Mechanical milling
Hydrogen storage dynamics
Activation energy

ABSTRACT

In this paper, we applied ball milling technique to prepare amorphous and nanocrystalline $CeMg_{11}Ni + x$ wt.% Ni ($x = 100$, 200) alloys which gaseous and electrochemical hydrogen storage dynamics and structure characteristics were systematically studied. It is shown that increasing Ni proportion promotes the amorphization of alloys, meanwhile, it improves their gaseous and electrochemical hydrogenation dynamics significantly. Besides, adjusting milling duration markedly changes the hydrogen storage performances. With the prolonging of milling time, the hydrogen storage capacity has a maximal value, which are 5.949 wt.% and 6.157 wt.% respectively for $x = 100$ and 200 alloys, while the dehydriding rate always increases. The hydriding rate and high rate discharge ability have the maximal values with the variation of milling time as well. The improved gaseous hydrogen storage dynamics is convinced to be connected with the reduction of dehydrogenation activation energy resulted by increasing Ni proportion and prolonging milling duration.

1. Introduction

The more and more serious environmental problems, especially the greenhouse effect resulted by consuming the limited fossil fuels, have attracted attention all over the world. Transport consumes about 25% energy of the world each year [1]. Also, automobile exhaust has been confirmed as the chief culprits of the severe haze in Beijing, which is declared by the Ministry of Environmental Protection of China recently. Therefore, developing a cleaner and renewable energy source is proposed as a promising strategy to reduce the fossil fuels consumption. Hydrogen energy is featured by the outstanding peculiarities, including inexhaustible supply, high energy efficiency and none-pollution and it has been treated as one of the most helpful choices among a mass of possible energy sources [2,3]. Nowadays, the main technical obstacle to apply hydrogen to clean energy vehicles, including hydrogen fueled vehicles, onboard fuel-cell, hybrid electric vehicle (HEV) and electric vehicle (EV), is believed to build a practical hydrogen storage system [4]. Storing hydrogen in metal hydrides is regarded as one of the preferential realized methods, which meet all requirements of mobile application, among hydrogen storage methods [5]. Recently, varies metal hydrides have been investigated as potential hydrogen storage systems, some of which even have been applied practically [6–8]. However, no one could meet the property requirement of vehicular application that the U.S. Department of Energy (DOE) suggested [9,10]. A lot of studies of applying hydrogen storage materials to Ni-MH battery as negative electrodes have been done. Thereinto, rare earth based AB_5 and AB_2 type alloys even have been large-scale commercialized, though both of them are unsatisfactory as the electrode materials applied to EV or HEV because of their relatively low specific capacity. Concerning hydrogen absorption capacity, Mg-based hydrogen storage alloys are considered as a promising material for hydrogen fuel-cell vehicle or negative electrode in Ni-MH battery [11]. Recently, Yuan et al. [12,13] investigated the structure, hydrogen storage kinetics and thermodynamics of Mg-base Mg-RE binary alloy. The hydrogen storage properties of Mg_3M also been reported [14,15]. $REMg_{12}$-type alloys have a theoretical electrochemical capacity of over 1000 mAh/g

---

[*] Corresponding author. Department of Functional Material Research, Central Iron and Steel Research Institute, No. 76 Xueyuannan Road, Haidian District, 100081 Beijing, PR China.
E-mail address: zhangyh59@sina.com (Y. Zhang).

https://doi.org/10.1016/j.renene.2018.07.134

[16] and a gaseous hydrogen storage capacity of 3.7–6.0 wt.% [17], there are many researchers paying much attention on them. Meanwhile, we cannot ignore their imperfections, including high dehydrogenation temperature, poor dynamic property and low electrochemical discharge capacity at room temperature. Thus, there are still many challenges for researchers to overcome to realize the commercialization of Mg-based alloys as hydrogen storage material on-board or negative electrode material in Ni-MH battery.

Alloying and microstructure modification are two accepted effective methods to improve hydrogen storage properties of the alloys [18]. Many reports point out that partially replacing Mg by rare earth elements can decrease the stability of Mg-based hydrides and facilitate the dehydrogenation property [19–21]. Meanwhile, this replacement can also prevent the corrosion of alloys and improve the cycle stability of the alloy [22,23]. Moreover, the structure of Mg-based alloys has a great influence on their hydriding and dehydriding dynamics [24]. When the grain size reduces to far below micrometer scale, their hydrogen absorption and desorption properties will be increased obviously [25]. Révész et al. [26] improved the hydriding/dehydriding properties of Mg_2Ni by generating nanocrystalline trough high-pressure torsion. Wu et al. [27] found that amorphous and/or nanocrystalline Mg–Ni-based alloys have a high electrochemical hydrogen capacity even at room temperature. To prepare amorphous and nanocrystalline Mg-based alloys, many techniques have been used, including rapid solidification (RS) [28], mechanical milling [29], equal channel angular pressing (ECAP) [30], hydriding combustion synthesis [31] and so on. Among them, melt spinning and mechanical milling are two widely accepted effective techniques, which can distribute elements homogeneously. Huang et al. [32] utilized melt spinning to prepare an amorphous and nanocrystalline $Mg_{65}Ni_{27}La_8$ alloy, and found it has the highest discharge capacity of 582 mAh/g at room temperature. Wu et al. [33] prepared $Mg_{20}Ni_8Mn$ alloys with microcrystalline, nanocrystalline, and amorphous microstructures by changing the velocity of copper wheel from 3.1 to 20.9 m/s during rapid solidification. Wang et al. [34] prepared ball milled $MmMg_{12}$ alloy with Ni powders, and found that adding Ni proportion from 150 to 200 wt.% leads to an increase of first discharge capacity from 770 to 1200 mAh/g. Yuan et al. [35] milled Sm_5Mg_{41} with CoS_2 powder and reduced its dehydriding activation energy from 128.19 kJ/mol to 95.49 kJ/mol. Zhang et al. [36] prepared $Mg_{10}NiR$ ($R = La$, Nd and Sm) alloys by melt spinning and found these alloys have superior hydrogenation and dehydrogenation dynamics because of the addition of various rare earth elements.

In this experiment, Ni was added to replace the Mg in $CeMg_{12}$-type alloy partially. We prepared the amorphous and nanocrystalline $CeMg_{11}Ni + x$ wt.% Ni ($x = 100, 200$) alloys with mechanical milling technique, and investigated their gaseous and electrochemical hydrogen storage properties influenced by Ni content and milling duration systematically.

2. Experimental

$CeMg_{11}Ni$ alloy was smelted by a vacuum induction furnace, which is filled with a 0.04 MPa helium atmosphere for preventing Mg from volatilization. The sources of block metal simple substance Ce, Mg, and Ni are CISRI corporation, and their purities are at least 99.99%. By pouring the molten alloy into a copper mould we got the cast ingots. The ingots were crushed into powder with 50 μm in diameter and mixed with Ni powder (CISRI Corporation, 50 μm in diameter, purity of 99.99%) with the weight ratios of 1:1 and 1:2 respectively. And then, we milled the mixed powders through a planetary-type mill and handled the as-milled sample alloys in an Ar-filled glove box which can protect the powder from being oxidized. The mill vials and balls were made of Cr-Ni stainless steel. The ball to powder mass ratio was 35:1 with the revolving speed setting at 135 rpm for different milling durations of 5, 10, 20, 40 and 60 h, respectively.

To study the phase composition, the alloy powders were tested by X-ray diffraction (XRD) (D/max/2400), which radioactive source was $CuK_{\alpha1}$ and filtered by graphite, at 40 kV, 160 mA and 10 °/min. To study the microstructural and crystalline states, the sample powders were observed through high resolution transmission electron microscope (HRTEM) (JEM-2100F, operated at 200 kV) and electron diffraction (ED).

De-/hydrogenation dynamic and thermodynamic performances of the alloys were investigated by an automatically controlled Sieverts apparatus, the temperature accuracy of which is ±2 K. 300 mg sample powder was weighted out for each test and subjected to five times hydriding/dehydriding cycles with the hydrogenation reaction occurring at 613 K and 3 MPa and the dehydrogenation reaction occurring at 613 K and 1×10^{-4} MPa. Thus performance stability can be remained [12,13]. The hydrogenation and dehydrogenation processes were measured at 553, 573, 593 and 613 K with the initial pressure setting at 3 and 1×10^{-4} MPa respectively. The weight of added Ni powder has not been taken into account in gaseous hydrogen absorption and desorption capacities. Thermal gravity analysis (TGA, Q600) was also sued to measure the dehydrogenation performance with heating rates setting at 5, 10, 15 and 20 K/min. In addition, the uncertainties have been estimated, including measurement error and calculation error. The hydrogen desorption kinetics measuring experiments and their verifying experiments show that the measurement error are less than 0.5%, respectively. The calculation error is less than 0.1%.

A tri-electrode open cell was utilized at 303 K to measure the electrochemical dynamics of sample alloys. The cell was equipped with one working electrode (sample alloys), one counter electrode (sintered $Ni(OH)_2/NiOOH$), one reference electrode (Hg/HgO), and electrolyte of 6 mol/L KOH. In each charging/discharging cycle, we charged the cell at a constant current density at first, after which and 15 min rest we discharged it at the same current density till the cut-off voltage of −0.500 V.

Electrochemical workstation (PARSTAT 2273) was utilized for measuring the electrochemical impedance spectra (EIS) at different temperatures. The EIS was tested at a 50% depth of discharge (DOD), the frequency ranged from 10 kHz to 5 mHz, and the amplitude of potential disturbance was 5 mV. The potentiostatic discharge was measured by discharging a fully charged electrode at 500 mV for 5000 s, which was controlled by an electrochemistry corrosion software (CorrWare) on electrochemical workstation.

3. Results and discussion

3.1. Microstructure

The XRD curves of the as-cast and milled $CeMg_{11}Ni + x$ wt.% Ni ($x = 0, 100, 200$) alloys before and after hydrogen absorption are shown in Fig. 1. The XRD curves of as-cast $CeMg_{11}Ni$ alloy clearly show that this alloy contains two phases, including $CeMg_{12}$ as a major phase and Mg_2Ni as a secondary phase. After ball milling, the XRD curves merge and broaden obviously, suggesting the nanocrystallization or non-crystallization of the crystalline alloys caused by ball milling. Moreover, the diffraction peaks of Ni added alloys become weaken and widen, the tendency of which becomes more obvious with Ni content increasing. This phenomenon reflects the facilitation of the non-crystallization of alloys resulted by adding Ni content, just as Abdellaoui et al. [37] stated that adding Ni proportion will lower the activation energy for crystalline phases in